Portable, tunable, high-luminosity spherical crystal spectrometer with an x-ray charge coupled device, for high-resolution x-ray spectromicroscopy of clusters heated by femtosecond laser pulses

Cite as: Review of Scientific Instruments **72**, 1956 (2001); https://doi.org/10.1063/1.1355273
Submitted: 24 October 2000 • Accepted: 24 January 2001 • Published Online: 27 March 2001

F. Blasco, C. Stenz, F. Salin, et al.

Portable, tunable, high-luminosity spherical crystal spectrometer with an x-ray charge coupled device, for high-resolution x-ray spectromicroscopy of clusters heated by femtosecond laser pulses

F. Blasco,[a] C. Stenz, and F. Salin
Laboratoire CELIA, CNRS-Université Bordeaux 1, UMR 5107, 33405 Talence, France

A. Ya. Faenov, A. I. Magunov, T. A. Pikuz, and I. Yu. Skobelev
Multicharged Ions Spectra Data Center of VNIIFTRI, Mendeleevo, Moscow region 141570, Russia

(Received 24 October 2000; accepted for publication 24 January 2001)

A portable ($200\times100\times100\,\mathrm{mm}^3$), high-luminosity, spherically bent crystal spectrometer was designed for measuring in a wide spectral range of 1.2–19.6 Å very low emissivity x-ray spectra of different clusters heated by 35 fs laser radiation. This spectrometer is associated with a custom design x-ray charge coupled device that features a large sensitive area ($24.6\times24.6\,\mathrm{mm}^2$) and a small pixel size ($24\times24\,\mu\mathrm{m}^2$). This apparatus provides simultaneous high spectral ($\lambda/\delta\lambda\sim1000-5000$) and spatial (40–80 μm) resolution. A large ($30\times10\,\mathrm{mm}^2$) open aperture mica crystal with $R=100$ mm is used as the dispersive and focusing element. The large tuneability of the spectrometer makes it possible to record high-resolution spectra of H-like ions of oxygen (CO_2 clusters) in a spectral range of 15–17 Å, Ne-like like ions of Kr in a spectral range of 5–5.7 Å, and He-like spectra of Ar in a spectral range of 3.0–3.4 and 3.7–4.4 Å without any adjustment of the spectrometer setup. Thanks to the high luminosity (high collection efficiency) of the spectrometer, high quality spectra were obtained using only 15 mJ 2000 laser shots. © *2001 American Institute of Physics.* [DOI: 10.1063/1.1355273]

I. INTRODUCTION

The investigation of ultrashort laser pulse radiation interaction with solid, gas, and cluster targets has received great interest in recent years. Such studies, on the one hand, give knowledge about fundamental properties of matter under critical conditions. On the other hand, they provide new solutions for different applications such as ignition of nuclear reactions, heavy particle acceleration, construction of bright x-ray sources for medicine, biology, and lithography, and others. Regardless of the kind of target (gas, liquid, cluster, or solid) interaction with a subpicosecond laser pulse induces a plasma which becomes a bright source of x rays. The main features of the plasmas are revealed in their emission spectra and x-ray spectroscopy is intensively used for femtosecond- and picosecond laser-produced plasma studies. The results with ultrashort pulses already obtained showed the dominant role of processes that were of less importance for plasma created by nanosecond or tens of picosecond laser pulses. Among the different targets clusters are especially interesting for the investigation of femtosecond laser interaction with matter, due to their very high efficiency at absorbing laser energy and their transformation into strong x-ray radiation and high energy multicharged ions (see, for example, Refs. 1–11).

The x-ray emission spectra from clusters heated by fs laser radiation have often been measured using flat crystal spectrometers.[1,12–18] The quality of the measurements is generally not very high due to the poor luminosity of flat crystal spectrometers and to the weak intensity of femtosecond laser-produced plasma x-ray radiation in the spectral range below 20 Å. For increasing x-ray detection efficiency von Hamos spectrometers with mica crystals[19,20] have been used, which has allowed one to obtain Ne-like ion spectra of Xe clusters.

Very important information about different spatial regions of the plasma from which the x-ray spectra are emitted could be obtained if a slit, placed perpendicular to the spectral dispersion of the crystal, is used. Unfortunately, the slit also decreases the throughput of the spectrometer. Recently, spectra from clusters heated by 60 fs high-intensity laser radiation have been measured[5,8,10,11] with simultaneously high spectral ($\lambda/\delta\lambda\sim5000-10\,000$) and spatial ($\sim10-30$ μm) resolution using a focusing spectrometer with spatial resolution in one dimension (1D) and in two dimensions (2D) (FSSR-1, 2D), based on a spherically bent crystal with a large open aperture and small radius of curvature.[21–24] The advantage of this apparatus is the absence of any slit, while providing both spectral and spatial resolution. High spectral and spatial resolution as well as high luminosity are achieved for FSSR-1, 2D spectrometers using the focusing properties of spherically bent crystals. Unfortunately, in most experiments these spectrometers were used in conjunction with photographic films as a detector. This prevented us from receiving real time information during the experimental run.

At the same time in past few years very effective x-ray charge-coupled devices (CCD) have been developed. The advantages of the combination of a FSSR-1, 2D spectrometer with such an x-ray CCD were successfully demonstrated in high-resolution x-ray spectromicroscopy investigations using

[a]Electronic mail: blasco@celia.u-bordeaux.fr

the Tokyo electron beam ion trap x-ray source.[25] However, this particular x-ray CCD required nitrogen cooling and could not be placed inside a vacuum chamber, where the x rays were produced, which is not very convenient for typical laser-produced plasma experiments.

More portable x-ray CCDs, like the Princeton x-ray CCD,[26] were developed recently and have started to be used effectively for measurements of x-ray radiation properties in laser-produced plasma experiments.[26–32] Such CCDs have very high luminosity over a wide spectral range and good enough (24 μm) spatial resolution. Another very important point for femtosecond laser-produced plasma investigations in which the intensity of x-ray laser radiation is weak is the small size of the Princeton CCD and the possibility of using it inside the experimental vacuum chamber close to the target area.

In this article we present details of the construction and the initial results obtained with a portable, tunable, high-luminosity x-ray spectrometer based on a spherically bent mica crystal and an x-ray CCD. The combination of FSSR-1, 2D spectrometers and an x-ray CCD additionally increases the luminosity and flexibility of such devices and makes it possible to record new information about femtosecond laser interaction with a wide variety of clusters.

II. SPECTROMETER CONFIGURATION

A. Geometry of a spherically curved crystal x-ray spectrometer

FSSR-1, 2D spectrometers utilize both the focusing aspects of the spherical mirror configuration as well as Bragg crystal x-ray diffraction and must satisfy both conditions simultaneously. The main properties of spherically bent crystal could be explained using two independent mutually perpendicular planes: (1) a *horizontal* or *meridional* or *dispersive* plane and (2) a *vertical* or *sagittal* or *focusing* plane.

Since the crystal itself does not have any specific geometrically determined plane, the first one can be defined by the position of the source, the detector, and the crystal. The second one is just perpendicular to the first one.

Let us consider the rays in the meridional plane shown in Fig. 1, where a is the distance from the source to the crystal, b is the distance from the crystal to the image, and R is the crystal bending radius. The glancing angle Θ of the radiation at the crystal is related to the wavelength λ by the Bragg condition,

$$2d_n \sin\Theta = n\lambda, \tag{1}$$

where n is the diffraction order; d_n is the interplanal distance for the nth diffraction order.

After reflection from the crystal, spectrally selected beams are formed in the meridional plane. Due to astigmatism, these beams are focused at different points in the meridional and sagittal planes. The positions of these points are given in the sagittal plane by

$$1/a + 1/b_s = (2\cos\varphi)/R, \tag{2}$$

and in meridional plane by

$$1/a + 1/b_m = 2/(R\cos\varphi), \tag{3}$$

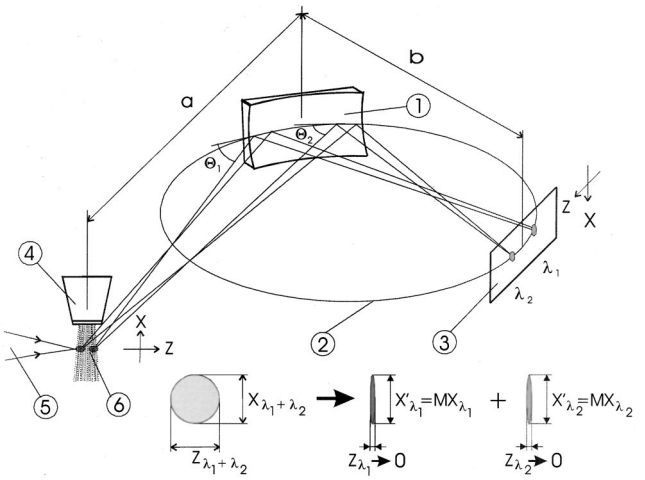

FIG. 1. Optical configuration of the FSSR-1D spectrometer using a spherically bent crystal. (1) Spherically bent crystal, (2) Rowland circle, (3) detector, (4) gas jet, (5) laser beam, (6) laser-produced plasma. *a*: Distance between the plasma and the spherical crystal; *b*: distance between the spherical crystal and the x-ray CCD detector. At the bottom, the transformation of the polychromatic x-ray plasma source configuration to a one-dimensionally spatially resolved monochromatic image is shown.

where b_s and b_m are the distances from the crystal to the points of sagittal and meridional beam focusing, R is the radius of curvature of the crystal, and $\varphi = 90° - \theta_B$ is the angle of incidence (from normal incidence) of the incoming radiation.

To achieve the best possible spatial resolution and the best possible intensity in the image we must place the film or the CCD exactly at distance b_s from the crystal in accordance with Eq. (2). In the case of the FSSR-1D spectrometer the x-ray detector must be placed on the Rowland circle in order to obtain good spectral resolution (in analogy to the classical Iohann type scheme for a cylindrically bent crystal). It follows that, in order to obtain good spatial resolution perpendicular to the detector dispersion plane, the source must be set up at a distance

$$a = R\cos\varphi/\cos 2\varphi \tag{4}$$

from the crystal and the detector at a distance

$$b = b_s = R\cos\varphi \tag{5}$$

from the crystal. As a result we have in the meridional plane one-dimensional spectrally selected images of plasma sources with linear magnification in the sagittal direction M. Magnification is given by $M = b/a = \cos 2\varphi$ (see Fig. 1).

In the case of the FSSR-2D spectrometer, the detector could be placed in any position with regard to the Rowland circle, but Eq. (2) must still be satisfied. For example, if distance $a = R\sin\varphi$ (the source is on the Rowland circle), then

$$b = b_s = R\cos\varphi/\cos 2\varphi. \tag{6}$$

In such a scheme, the linear magnification in the sagittal plane is given by $M = 1/\cos 2\varphi$. In order to get a fast estimate of the spectral resolution, which can be obtained for the optical systems of FSSR-1D and FSSR-2D spectrometers in MISDC, a ray-tracing package has been developed.[33]

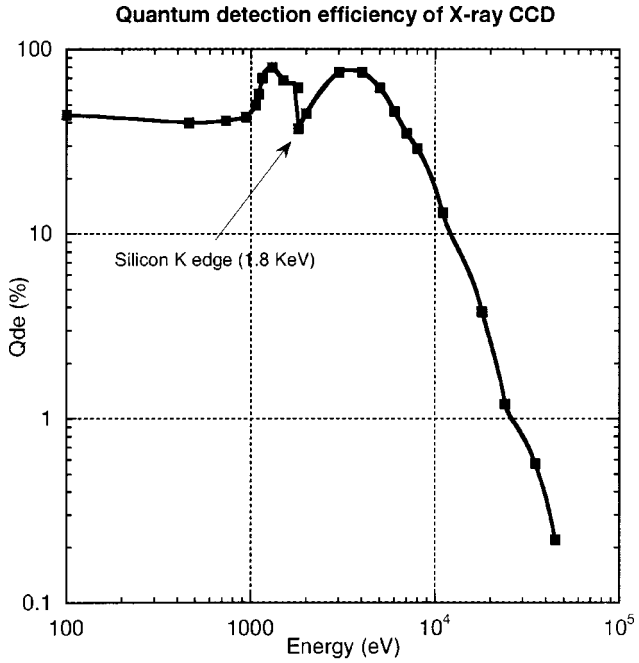

FIG. 2. Quantum detection efficiency of the Princeton Instruments x-ray CCD (Refs. 27–31) vs photon energy.

B. X-ray camera description

A description of the vacuum compatible, miniature camera was reported few years ago in Ref. 27. As was shown in Refs. 28–31 the x-ray CCD camera[26] is vacuum compatible and can be positioned very close to the target area even inside a small experimental vacuum chamber. The main characteristics of this low noise and high dynamic range camera were described in Refs. 28 and 30. The combination of superior spatial resolution, low inherent noise, excellent linear response, and high quantum detection efficiency have made CCDs very attractive detectors compared to x-ray films and other photoelectric detectors for two-dimensional imaging. This x-ray CCD camera covers the x-ray range from 100 eV to 50 keV with very good quantum detection efficiency as shown in Fig. 2.

The $60\times60\times80\,\mathrm{mm}^3$ camera uses a backilluminated CCD array (SITe TK 1024×1024).[32] The sensor is in thermal contact with the cold side of a two-stage Peltier thermoelectric cooler which typically can be operated at temperatures between -30 and $-50\,^{\circ}\mathrm{C}$. The hot side of the Peltier thermoelectric cooler is attached to a heat sink. The heat from the Peltier stack can be removed by continuously flowing $10\,^{\circ}\mathrm{C}$ water into the copper block. Cooling the camera to $-45\,^{\circ}\mathrm{C}$ takes 15 min. The camera can operate for long periods in vacuum. The CCD array is composed of 1024×1024 pixels. Each pixel is $24\times24\,\mu\mathrm{m}^2$, providing an active area of $24.6\times24.6\,\mathrm{mm}^2$.

The removable CCD front window can be replaced by metallic filters for x-ray detection. The front chamber of the CCD is pumped in order to prevent water condensation damage on the cooled CCD sensor. The on-board electronics are connected to an external controller (Princeton Instruments ST138). The signal is converted by a high-resolution 16-bit converter analog to digital (ADC). The CCD camera controller operates continuous cleaning of the CCD until a trigger signal is received. This prevents buildup of dark current and unwanted signals prior to the x-ray pulse. Readout can follow immediately after the trigger signal. All the camera specifications are summarized in Refs. 28–30.

C. Spectrometer setup

Large open aperture spherically bent crystals of mica with different radii of curvature $R=100$, 150, and 250 mm and differently oriented quartz crystals with $R=150$ and 250 mm are produced routinely at the Multicharged Ions Spectra Data Center of VNIIFTRI (Russia). Spherical crystals were produced by standard bending between two substrates with certain radius of curvature and fixed by glue on the concave substrate.[38–41] For purposes of the present experiment (registration of weak x-ray spectra) it was necessary to increase the spectrometer's luminosity. In such a case the distance between the crystal and the plasma must be as small as possible and we chose spherically bent mica crystals with a minimum radius of curvature ($R=100\,\mathrm{mm}$). The size of the spherically bent mica crystal was $30\times10\,\mathrm{mm}^2$. One big advantage of mica crystals is their very good reflectivity in different diffraction orders. In practice, it is possible to observe spectra in I, II, III, IV, V, VII, VIII, XI, XII, and XIII diffraction orders. Since the lattice space of mica crystal in the first order of diffraction is $2d\approx19.91$ Å, it becomes possible to cover a very wide spectral range from about 1.2 up to 19 Å and thus to measure x-ray spectra from targets with very different nuclear charges Z using only one spectrometer and even one alignment.

As was mentioned above, the intensity of x-ray emission of clusters heated by femtosecond laser radiation is very weak. To minimize the distance between the crystal and the plasma source, the spherical crystal was mounted on a specially designed minispectrometer body [see the schematic in Fig. 3(a) and the photo of the spectrometer in Fig. 3(b)], which included three minigoniometers. These minigoniometers are necessary for precise alignment of FSSR-1, 2D spectrometers according to the results of ray-tracing calculations. The x-ray CCD was also mounted on this spectrometer body. It is possible to move the CCD on the spectrometer body to cover a wider spectral range using a lower order of diffraction. We would like to emphasize that the overall size of the spectrometer is very small and does not exceed $200\times100\times100\,\mathrm{mm}^3$.

Alignment of the FSSR-1, 2D spectrometer is done in three stages. First, the angles and distances in the spectrometer body are set according to the results of the ray-tracing program for the specific experiment. Then, the whole aligned spectrometer body is placed inside the vacuum chamber in such way that the distance between the crystal and target corresponds to the distance calculated by the ray-tracing program.[33] Finally, the overall quality of the alignment is checked with a He–Ne laser using some analogies between reflections of x-ray radiation and visual light. A visible point source is put in the plane of the x-ray source. At this stage it is necessary to obtain in the plane of the detector a line as narrow as possible.

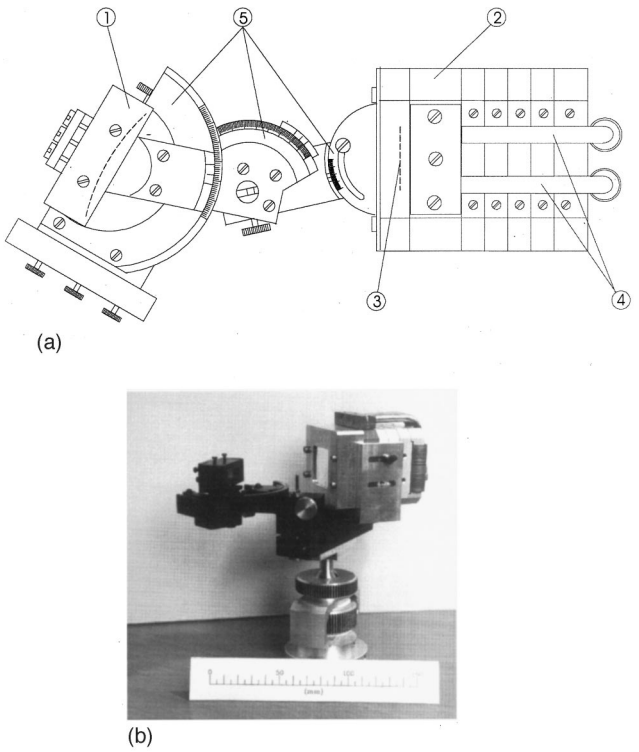

FIG. 3. (a) Schematic of a spherical spectrometer with an x-ray CCD detector: (1) Spherically bent crystal, (2) x-ray CCD holder, (3) x-ray CCD sensitive chip, (4) cooling tubes of the CCD, (5) minigoniometers. (b) Photo of the spherically bent crystal spectrometer.

In real experiments the spectrometer can be used at Bragg angles between 45° and 75°. This means that, using different diffraction orders of the mica crystal, it is possible to measure spectra in a very wide spectral range, 1.2–19.6 Å.

The total spectral resolution of the spectrometer is given by the following conditions.

(1) The intrinsic spectral resolution of the crystal is due primarily to imperfections in the crystalline lattice. It is well known that mica is not a perfect crystal, but as was shown experimentally and theoretically in Refs. 34 and 35 the spectral resolution $\lambda/\delta\lambda$ can reach values higher than 1000 for wavelengths around 19 Å and about 10 000 for wavelengths smaller than 10 Å. Furthermore, in this work we demonstrate experimentally and theoretically that the spectral resolution does not decrease in the case of precise bending of the crystals on the spherical curvature even with very short radius of $R=100$ mm.
(2) The spectral resolution due to the quality of detector. In our case the pixel size of the CCD was 24 μm. It means that for typical dispersion of the spectrometer of around 0.02–0.04 Å/mm for a spectral range about 3–4 Å, the spectral resolution is limited by the quality of the x-ray CCD detector and corresponds to $\lambda/\delta\lambda\approx 5000$. For the spectral range of 5–6 Å, the dispersion is 0.05–0.06 Å/mm and the resolution is $\lambda/\delta\lambda\approx 4400-5000$. For spectral range of about 14–17 Å, the dispersion is 0.14–0.17 Å/mm and the resolution is $\lambda/\delta\lambda\approx 4000-4500$.
(3) The spectral resolution due to the size of the plasma x-ray source was demonstrated in Ref. 24; the spectral resolution in the case of a detector located on the Rowland circle (FSSR-1D) is not limited by the source size. In this article, we also considered the possibility of placing the detector outside the Rowland circle. It was demonstrated that, even in such a case, spectral resolution $\lambda/\delta\lambda\approx 5000$ could be achieved for typical sizes of the laser-produced plasma x-ray source of about 50–500 μm.

Thus, for a spectral range of about 10–19 Å, the spectral resolution of our spectrometer is limited by the intrinsic resolution of the crystal and can reach $\lambda/\delta\lambda\approx 1000-4500$; at the same time for wavelengths shorter than 10 Å, it is limited to $\lambda/\delta\lambda\approx 5000-6000$ because of the size of the CCD pixels. The actual spectral resolution must also include the contribution due to different broadening of the spectral lines. In laser-produced plasma experiments, the resolving power of individual lines ($\delta\lambda/\lambda\approx 1000-2000$) is limited by these broadenings.

One very big advantage of FSSR-1, 2D spectrometers is the possibility of obtaining simultaneously high spectral resolution and high spatial resolution due to the focusing properties of the spherically bent crystal. The spatial resolution of our spectrometer is about 40–80 μm and is determined by the optimal focusing conditions.

Three sets of test experiments were conducted in order to demonstrate the performance of the FSSR spectrometer associated with the x-ray CCD detector.

III. FEMTOSECOND LASER FACILITY AND THE EXPERIMENTAL SETUP

The experiments reported here were carried out on the laser facility[36] at CELIA (Bordeaux, France). The laser source produces terawatt level femtosecond pulses at a 1 kHz repetition rate. A Ti:sapphire oscillator produces 10 fs pulses which are amplified in a series of four amplifiers. Chirped pulse amplification is used to avoid any damage in the chain. All four Ti:sapphire amplifiers are pumped by five Nd:YLF lasers running at 1 kHz. The pulse energy is about 20 mJ around 800 nm, and the pulse duration can be adjusted from 20 fs to several picoseconds. Pre-pulse formation in the regenerative amplifier several nanoseconds before the main pulse causes destruction of the clusters,[11] and has been prevented by using a Pockels cell. A contrast ratio of better than 10^6 is obtained. The measured ASE background intensity is at least eight orders of magnitude less than the laser pulse intensity. The pulse-to-pulse stability of our laser source was typically 2% root mean square (rms).

To avoid self-focusing of the beam, and also damage to the compressor, the laser beam propagates in vacuum. The maximum available energy on the target is about 15 mJ. A 6 μm laser spot radius is obtained in vacuum by using a 75 mm focal length, $f/2$ off-axis parabolic mirror. The maximum laser intensity on the target is 4×10^{17} W/cm^2.

Ar, Kr, and CO_2 cluster targets are produced in the vacuum chamber using a fast pulsed supersonic gas jet. The radial distribution and the mean size of the clusters, in expanding flow, are obtained by Rayleigh scattering measurements.[37] The laser pulse was focused onto the gas jet

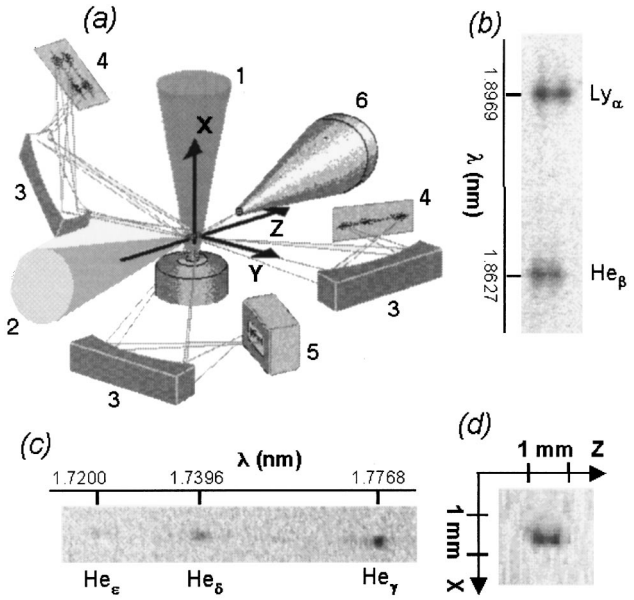

FIG. 4. (a) Experimental setup: (1) Expanding jet of clusters, (2) laser beam, (3) focusing spectrometers with mica crystals with $R=150$ and 100 mm, (4) RAR-2492 or DEF films, (5) Princeton Instruments x-ray CCD, (6) pinhole camera. (b) Spectrogram from a spectrometer with a spatial resolution along the axis of the laser beam (spectral resolution perpendicular to the laser propagation). (c) Spectrogram from a spectrometer with a spatial resolution across the jet axis (spectral resolution along laser propagation). (d) X-ray pinhole image of the plasma.

at a distance of 1.5 mm from the nozzle output. The diameter of the cylindrical output nozzle is 2.5 mm and the velocity of the particles is Mach 2.5. The divergence of the gas jet is about 22°. The maximum backing pressure in the fast valve is 80 bar. During this experiment it was not possible to run the jet continuously while keeping the vacuum below 10^{-2} mbar. The jet was pulsed for 50 ms at a 1 Hz repetition rate (5% duty cycle). With respect to the 1 kHz repetition rate of the laser, this corresponds to an effective repetition rate of 50 Hz. Improvement of the pumping system in the future should make it possible to run the x-ray source close to the 1 kHz maximum rate.

The experimental setup for x-ray registration is shown in Fig. 4. The nonspectrally resolved ''pinhole camera'' image of the x-ray plasma source was obtained by using a 10 μm diam pinhole. The imaging magnification was about 2.1, corresponding to a resolution of around 10 μm on the target and was adjusted to the maximum resolution of a 1024×1024 pixel x-ray CCD. The x-ray CCD camera is cooled down to -45 °C. Each pixel is 24×24 μm wide and detects photons ranging from visible to x ray (0.1 nm). A filter in front of the x-ray CCD camera is used to prevent it from any damage due to the main beam or the visible radiation. The filter is a 2μm polypropylene layer coated on both faces by a 0.4 μm aluminum layer. Only photons with energy above 200 eV can be detected. The angle between the laser beam axis and the imaging axis of the pinhole was 20.5°.

IV. EXPERIMENTAL RESULTS

A typical pinhole image is presented in Fig. 4(d). One can clearly see, in the direction of the laser propagation, two hot spots of practically identical size. The x-ray emission has approximately the same intensity for both. At the same time, perpendicular to the laser direction, we observed only one region of x-ray radiation of about 300–400 μm.

X-ray spectra were recorded using an x-ray spectrometer with a spherically bent mica crystal ($R=100$ mm), followed by an x-ray CCD detector. Parallel to this spectrometer, two additional spectrometers with spherically bent mica crystals ($R=150$ mm) recording the x ray on the films were placed in the vacuum chamber. A schematic of this experimental arrangement is shown in Fig. 4. The observation angle of the spectrographs was about 70°–110° to the laser beam propagation axis, which provides spatial resolution either along this axis or perpendicular to it.

The spectral resolution of the spectrographs using films as detectors was about $\lambda/\delta\lambda=2000$ in the 15–19 Å spectral region (the first order of diffraction) and about $\lambda/\delta\lambda=4000$ for wavelengths shorter than 10 Å (in the second, third, fourth, and fifth orders of diffraction). The spectra were recorded on RAR-2492 and DEF films protected by a 2 μm polypropylene layer coated by 0.4 μm of aluminum filter. The spatial resolution of the FSSR-1, 2D spectrometers with films was about 20–40 μm and was mainly limited by the film scanner used to digitize the spectra. Typical spectra of different spectral lines of H-like and He-like ions of oxygen with 1D spatial resolution, obtained with film spectrometers oriented parallel and perpendicular to the laser propagation axis, are presented in Figs. 4(b) and 4(c). Figures 4(b) and 4(a) show clearly that the x-ray source has the same features, as mentioned before, with two separate hot spots with a total size emitting zone of about 1 mm in the laser propagation direction and one spot of about 300–400 μm in the perpendicular direction.

The spectrometer with a $R=100$ mm mica crystal and the CCD camera was tested in the FSSR-1D scheme (the sensitive plane of the CCD detector was located on the Rowland circle). The test experiments demonstrate that with one spectrometer alignment setup and using different diffraction orders of the mica crystal, it is possible to record simultaneously spectra of H-like ions of oxygen (CO_2 clusters), Ne-like ions of Kr clusters, and He-like ions of Ar clusters. To record these spectra simultaneously, a Bragg angle of $\theta=53.6°$ was selected for the spectrometer. A distance of $a=272.8$ mm between the crystal and the plasma was set according to our ray-tracing program. To eliminate the influence of the 1 mm x-ray source in the direction of laser propagation, we put the CCD camera on the Rowland circle. In this scheme the distance b between the crystal and film must be set equal to 50 mm($R/2$). For such an alignment the magnification of the image in the direction perpendicular to the spectral dispersion is 1/3.4 tm. This means that the spatial resolution of about 81 μm on the target is limited by the size of the CCD pixels (24 μm). The spectrometer was oriented so that the spatial resolution was in the direction perpendicular to the laser beam propagation axis [the same as in Fig. 4(c)]. We would like to emphasize once more, that, because of the location of the detector on the Rowland circle and despite the big size of the plasma in the direction of the laser

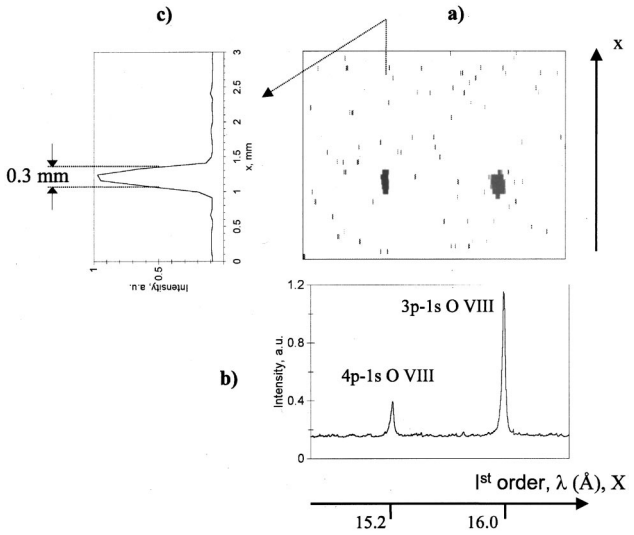

FIG. 5. Spectral images (a) of a 1D section in the direction of spectral resolution (b) and perpendicular (X according to Fig. 4) direction (c) for the case of CO_2 clusters, heated by 35 fs, 15 mJ pulses (over 2000 laser shots). The mica crystal was used in the first order of diffraction.

propagation, the spectral resolution was not limited by the size of the x-ray source.

The large size of our spherically bent crystal made it possible to measure spectra over wide spectral ranges: 15–17 Å in the first diffraction order of the mica crystal, 5.0–5.7 Å in the third order of diffraction, and 3.7–4.4 Å in the fourth order of diffraction. Furthermore, due to overlapping of the fourth and fifth diffraction orders, we could simultaneously obtain, on the plane of the detector, spectra in the spectral ranges of 3.7–4.4 and 3.0–3.4 Å (see Figs. 5–7). Thus, in one experiment we could simultaneously record spectra of the $Ly\alpha$ line of H-like ions of Ar and all lines of He-like ions of Ar up to the $K\alpha$ line. The spectral dispersion of the spectrometer was about 0.033 Å/mm for the spectral range around 4 Å (Ar lines), and the spectral resolution of $\lambda/\delta\lambda$

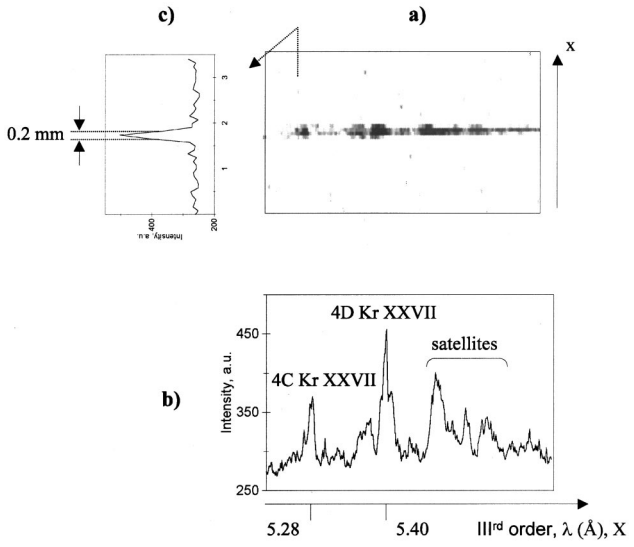

FIG. 6. Spectral images (a) of a 1D section in the direction of spectral resolution (b) and perpendicular (X according to Fig. 4) direction (c) for the case of krypton clusters, heated by 35 fs, 15 mJ pulses (over 2000 laser shots). The mica crystal was used in the third order of diffraction.

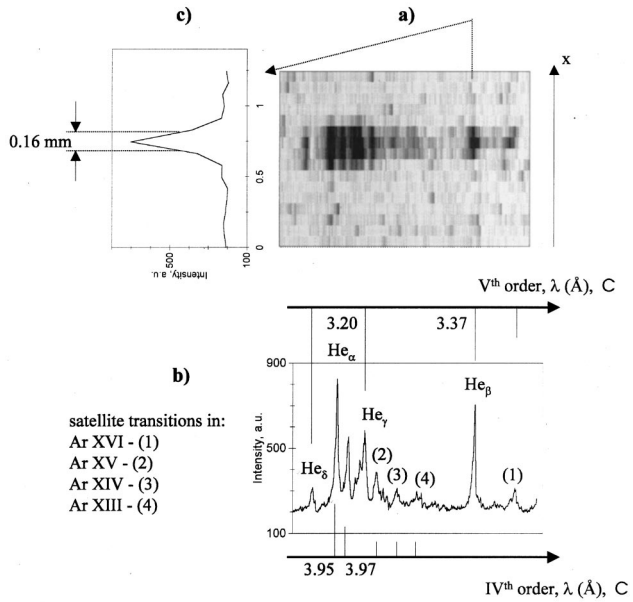

FIG. 7. Spectral images (a) of a 1D section in the direction of spectral resolution (b) and perpendicular (X according to Fig. 4) direction (c) for the case of argon clusters, heated by 35 fs, 15 mJ pulses (over 2000 laser shots). The mica crystal was used in the fourth and fifth orders of diffraction.

≈5000 was limited only by the CCD detector (pixel size). For a spectral range of about 5.3 Å (Kr lines) the spectrometer has dispersion of about 0.05 Å/mm and the resolution corresponds to $\lambda/\delta\lambda \approx 4400$. For a spectral range of around 16 Å (oxygen lines), the spectrometer dispersion was 0.15 Å/mm and the resolution $\lambda/\delta\lambda \approx 3000-4000$ was limited by the intrinsic resolution of the crystal.

Spectra produced by CO_2, Kr, and Ar clusters are given, respectively, in Figs. 5–7, and they were obtained using 35 fs, 15 mJ pulses from our Ti:sapphire laser. From these traces it is obvious that the very high spectral resolution of the spectrometer makes it possible to resolve very compli-

TABLE I. Comparison of luminosity of a flat KAP crystal spectrometer (Ref. 15) and a spherically bent mica crystal spectrometer (present work).

Laser source, Ti:S	Pulse duration (fs)	Pulse energy (mJ)	Peak intensity (W cm^{-2})	Cluster type	Ion	Spectral range (Å)	No. of shots
Ref. 15	90	50	1.4×10^{18}	Xe	Xe^{+27} Xe^{+35}	2.5–3.3	72 000
Ref. 15	90	50	1.4×10^{18}	Xe	Xe^{+26} Xe^{+}	9.5–15	18 000
This work	35	15	4×10^{17}	CO_2	O^{+7}	15–17	2000
This work	35	15	4×10^{17}	Kr	Kr^{+26} Kr^{+25}	5.0–5.7	2000
This work	35	15	4×10^{17}	Ar	Ar^{+16} Ar^{+10}	3.7–4.4 3.0–3.4	2000 (500)
This work	150	15	10^{17}	Ar	Ar^{+16} Ar^{+10}	3.7–4.4 3.0–3.4	2000
This work	500	15	2.7×10^{16}	Ar	Ar^{+16} Ar^{+10}	3.7–4.4 3.0–3.4	2000

cated satellite structures near He α and He β lines of argon He-like ions and Na-like satellites near resonance lines of Ne-like ions of krypton. These spectra are now being analyzed, and the results will be published at a later date. Figures 5–7 show the good focusing properties of the spectrometer. The dimensions of the x-ray emission zone of the plasma are very similar in pinhole images and spectral images. Because of the high luminosity of the FSSR-1D spectrometer, all spectra presented in Figs. 5–7 were obtained using 1 min laser exposure (2000 shots at a 50 Hz repetition rate). Furthermore, in some experiments high quality spectra in the vicinity of the He α line of argon were obtained using only 500 laser shots.

It is interesting to compare the luminosity of spectrometers previously used for obtaining x-ray spectra of clusters with the luminosity of the spectrometers presented here. For example, in Table I we compare our results with those obtained in a recent publication[15] in which a significantly more powerful Ti:sapphire laser was used to heat clusters observed with a flat x-ray spectrometer using a KAP crystal and film as the detector. The experiments presented here clearly demonstrate that, despite about 3 times smaller laser energy and 3–50 times smaller laser peak intensity, very good resolved spectra were obtained with 9–36 times less shots. It is also necessary to mention that in our experiments spectra were also obtained with spatial resolution while in previous experiments[15] spatial resolution was absent. We also would like once more to emphasize another important advantage of our spectrometer: its large spectral range. As a matter of fact, all the spectra presented in the spectral range of 3.0–17 Å were recorded with only one spectrometer alignment and no realignment.

ACKNOWLEDGMENTS

The authors would like to acknowledge the help of Jean Robert Roche and Alain Le Goff in setting up the experiment chamber. This work was supported by the Fond Européen de Développement Economique Régional and by the Conseil Régional d'Aquitaine.

[1] A. McPherson *et al.*, Phys. Rev. Lett. **72**, 1810 (1994).
[2] T. Ditmire *et al.*, Phys. Rev. A **53**, 3379 (1996).
[3] T. Ditmire *et al.*, Phys. Rev. Lett. **78**, 2732 (1997).
[4] M. Lezius *et al.*, Phys. Rev. Lett. **80**, 261 (1998).
[5] S. Dobosz *et al.*, JETP Lett. **68**, 454 (1998).
[6] J. Larsson and A. Sjogren, Rev. Sci. Instrum. **70**, 2253 (1999).
[7] J. W. G. Tisch *et al.*, Phys. Rev. A **60**, 3076 (1999).
[8] S. Dobosz *et al.*, JETP **88**, 1122 (1999).
[9] J. Zweiback *et al.*, Phys. Rev. Lett. **84**, 2634 (2000).
[10] T. Auguste *et al.*, JETP Lett. **72**, (2000).
[11] C. Stenz *et al.*, Quantum Electron. **30**, 721 (2000).
[12] K. Boyer *et al.*, J. Phys. B **27**, 4373 (1994).
[13] W. J. Blyth *et al.*, Phys. Rev. Lett. **74**, 554 (1995).
[14] A. McPherson *et al.*, J. Phys. B **29**, L291 (1996).
[15] K. Kondo *et al.*, J. Phys. B **30**, 2707 (1997).
[16] T. Ditmire *et al.*, J. Phys. B **31**, 2825 (1998).
[17] R. A. Smith *et al.*, Phys. Scr., T **T80**, 35 (1999).
[18] H. Honda *et al.*, Phys. Rev. A **61**, 23201 (2000).
[19] K. Boyer *et al.*, J. Phys. B **27**, 4373 (1994).
[20] W. A. Schroeder *et al.*, J. Phys. B **31**, 5031 (1998).
[21] A. Ya. Faenov *et al.*, Phys. Scr. **50**, 333 (1994).
[22] T. A. Pikuz *et al.*, X-Ray Sci. Technol. **5**, 323 (1995).
[23] I. Yu. Skobelev *et al.*, JETP **81**, 692 (1995).
[24] B. K. F. Young *et al.*, Rev. Sci. Instrum. **69**, 4049 (1998).
[25] N. Nakamura *et al.*, Rev. Sci. Instrum. **70**, 1658 (1999).
[26] Princeton Instruments, Inc., 3660 Quakerbridge Road, Trenton, NJ 08619.
[27] A. D. Conder *et al.*, Rev. Sci. Instrum. **66**, 709 (1995).
[28] J. Dunn *et al.*, Proc. SPIE **2654**, 119 (1996).
[29] J. Dunn *et al.*, Rev. Sci. Instrum. **66**, 706 (1995).
[30] J. Dunn *et al.*, Proc. SPIE **3301**, 100 (1998).
[31] L. Poletto *et al.*, Appl. Opt. **38**, 29 (1999).
[32] Scientific Imaging Technologies, Inc., P.O. Box 569, Beaverton, OR 97075.
[33] A. I. Magunov, A. Ya. Faenov, T. A. Pikuz, and I. Yu. Skobelev, Ray-tracing code for focusing spectrometers with spatial resolution (FSSR-1, 2D), MISDC, VNIIFTRI (1997).
[34] T. A. Pikuz *et al.*, Proc. SPIE **2515**, 468 (1995).
[35] G. Hoelzer *et al.*, Phys. Scr. **57**, 301 (1998).
[36] V. Bagnoud and F. Salin, Appl. Phys. B: Lasers Opt. **70**, 165 (2000).
[37] A. M. Bush, J. Phys. Chem. A **102**, 6457 (1998).
[38] V. A. Boiko *et al.*, J. Sov. Laser Res. **6**, 85 (1985).
[39] T. A. Pikuz *et al.*, Proc. SPIE **2279**, 244 (1994).
[40] T. A. Pikuz *et al.*, Proc. SPIE **2515**, 468 (1995).
[41] G. Hoelzer *et al.*, Phys. Scr. **57**, 301 (1998).